Application of Electrospinning to SiC Fiber Synthesis

Shao-Hwa Hu (3057816806@qq.com)
Dongguan Polytechnic https://orcid.org/0000-0001-6889-7350
Hang Dai
Dongguan Polytechnic
Li-Chun Wu
Dongguan Polytechnic
Ya-Zhao Ai
Dongguan Polytechnic

Research Article

Keywords: SiC fiber, polycarbosilane (PCS), dimethylformamide (DMF), electrospinning

Posted Date: April 20th, 2020

DOI: https://doi.org/10.21203/rs.3.rs-23086/v1

Abstract

Silicon carbide (SiC) possesses unique properties and is widely applied in household and military uses. This study explored the manufacturing process of SiC fibers. In the experiment, polycarbosilane (PCS) was dissolved in a mixed solvent of C8H10 and dimethylformamide (DMF) to form a solution, and electrospinning was employed to synthesize PCS fibers. PCS fibers underwent a curing process and a 2-h calcination at 1200°C in N2 atmosphere to convert PCS fibers into β-SiC fibers. The solute recruitment, solvent mixing ratio, and voltage in the experiment were defined as process parameters through which to examine the influence each parameter had on electrospinning. The PCS fibers were discovered to exhibit the most even size under the following condition: PCS recruitment of 1.0 g/ml, DMF constituting 30% of the solvent volume, voltage of 25 kV, spraying speed of 1.0 ml/h, and spinning distance of 15 cm. Under electron microscopy, the diameter of each PCS fiber was determined to be 1.0 μm, and the diameter of each β-SiC fiber was 0.8 μm.

1 Introduction

In 1978, Yajima et al. from Tohoku University first employed polycarbosilane (PCS) as a raw material [1] and applied melt spinning at a temperature ranging from 270°C to 350°C to obtain as-spun fibers. The as-spun fibers were then cured by heating them to 200°C in an aerobic condition, with temperature increasing at 30°C/h, and fibers were maintained at the temperature for 30 minutes. Subsequently, the fibers were heated again to 1300°C at a rate of 100°C/h, and then the fibers were maintained at that temperature for 60 minutes to synthesize silicon carbide (SiC) fibers [2, 3].

Yakima et al. stated that under thermogravimetric analysis, the weight of the as-spun fibers increased by approximately 8.0% after undergoing the curing process [2]. PCS fibers were fragile and less supportive; therefore, they were prepared through a curing process that stimulated the reaction between silicon in PCS and oxygen in the atmosphere. Si-O-Si bonds were then formed, generating an oxide coating (a high-melting-point coating) on the surface of the fibers that strengthened the fibers' function and enhanced the tensile strength. Accordingly, fibers were less likely to melt or break in the following calcination process, and SiC fibers could then be synthesized [4]. In the research conducted by Yajima et al., fibers were heated to 1300°C at a rate of 100°C/h and maintained at the temperature for 60 minutes in a vacuum condition or nitrogen flux. The process were divided into three phases: first, materials with low molecular weight became volatile or desorbed; second, PCS side chains pyrolyzed because of high temperature; third, the fibers in the polymer were converted to SiC and transformed from an amorphous form into crystalline β-SiC [5].

2 Experimental Process

2.1 Procedure

This study conducted the experiment by heating PCS to 200°C in a nitrogen flux and refining PCS at the constant temperature for 1 h to eliminate the low molecular weight polymer in PCS. On the basis of the approach offered in the literature [6–8], refined PCS was added into a mixed solvent of C_8H_{10} and dimethylformamide (DMF) to form a solution. Next, the solution was subject to electrospinning, curing, and calcination. Controlling the parameters in each procedure facilitated identifying the process parameters for producing SiC fibers with minimal wire diameters and consistent appearance. Fig. 1 and 2 display the experimental procedure and the diagram of the production.

2.2 Refinement of precursors

2.2.1 Weight of PCS precursors before and after refinement and a comparison using gel permeation chromatography

This study eliminated the polymers with low molecular weight in PCS precursors; therefore, prior to this study, precursors were heated to 200°C at a temperature incremental rate of 5°C/minute and held at this temperature for 60 minutes. The refining process is displayed in Fig. 3. After refinement, the PCS had a 9% weight loss.

According to the analysis using gel permeation chromatography (Fig. 4), before refinement, the weight average molecular weight (M_w) was 1181 Da, and the number average molecular weight (M_n) was 3401 Da. The polydispersity (M_n/M_w) was approximately 2.88. After refinement, the weight average molecular weight (M_w) was 1913 Da, and the number average molecular weight (M_n) was 4039 Da. The polydispersity (M_n/M_w) was approximately 2.11. In accordance with the aforementioned results, the molecular weights increased slightly, whereas the polydispersity decreased slightly.

2.2.2 Comparison of Fourier-transform infrared spectroscopy spectra before and after the refinement of PCS precursors

Fig. 5 presents the Fourier-transform infrared spectroscopy (FTIR) spectra before and after the refinement of PCS precursors. The two curves in this figure exhibit the identical shape, indicating that PCS did not bond with N_2 during refinement; only the evaporation of low molecular weight polymers were discovered. The stretching and flexural vibration of the Si-CH_3 bond corresponded to the peaks at 800 and 1250 cm^{-1}, the Si-CH_2-Si bond corresponded to that at 1020 cm^{-1}, and the Si-H bond corresponded to that at 2100 cm^{-1}; these peaks represent the characteristics of PCS.

2.2.3 ^{29}Si NMR differences before and after refinement of PCS precursors

As displayed in Fig. 6, two peaks were observed in both the curves before and after the refinement of PCS precursors. The absorption peaks at the −17 and 0 ppm chemical shifts represent the presence of SiC_3H and SiC_4, respectively [9]. The relative intensity of SiC_4/SiC_3H increased after refinement, indicating that

the amount of linear structures in low molecular weight SiC_3H decreased. The cross-link between PCS molecules was increased during refinement, indicating that refinement enhances precursor qualities.

2.3 Experimental design

After the refinement of PCS, two variables—namely the ratio of DMF added to the mixed solvent and the amount of PCS added to the solvent per milliliter—were defined and used to further determine which formula was most suitable for synthesizing fibers. Table 1 presents the experimental configuration of these two variables. Voltage was used as a parameter under constant extrusion rates and spinning distances to explore the influence of various voltage levels on fibers. Table 2 presents the configuration of this parameter. Concerning the curing process, the duration of temperature retention was used as the variable with which to inspect the influences of various durations of temperature maintenance on the fiber oxygen content. The experimental configuration of this variable is displayed in Table 3.

3 Results And Discussion

3.1 PCS solution preparation and spinnability analysis

3.1.1 Dissolution of PCS in various solvent formulas

The mixed solvents were prepared as designed. First, DMF and C_8H_{10} were blended according to the predetermined ratios and stirred with a magnetic mixer at 300 rpm for 1 h. Next, PCS was added to the mixed solvent, and the solution was placed in a thermostatic water bath under ultrasonic shock for 8 h at room temperature.

The results demonstrated that when the concentration of PCS exceeded 1.4 g/ml, the solution reached saturation and solute deposition was observed. Furthermore, when DMF accounted for more than 40% of the mixed solvent, PCS could no longer be completely dissolved, regardless of the amount added to the solvent, and solute deposition was also observed. This accords with the results of Yuan [8].

The solubility of PCS in each prepared solution is displayed in Fig. 7. The crosses represent situations where the solute could not be completely dissolved, and the circles indicate situations where solutes were completely dissolved. Solubility decreased with an increasing amount of DMF because of its inability to dissolve PCS.

The addition of DMF may benefit the spinning process [10] and reduce the formation of pores of the fiber surface because of its low volatility. To account for the importance of DMF in electrospinning, four solutions with relatively high amounts of DMF were selected (as shown in Fig. 7) to serve as specimens for the electrospinning experiment.

3.1.2 Viscosity in solution formulas

Electrospun fibers are easily affected by solution characteristics (viscosity, surface tension, polarity); therefore, four of the solution formulas were selected to perform a rheology experiment and examine the rheological characteristics of electrospun fibers. The results are displayed in Fig. 8.

As evident in Fig. 8, viscosity became high with an increase of PCS content. Under the same amount of PCS, the higher the amount of DMF taken up in a solvent was, the higher the solution's viscosity would become because the increase in DMF led to a decrease in C_8H_{10}. Because DMF is a type of polar solvent in which PCS cannot dissolve, the increase in DMF content signified less C_8H_{10} to dissolve PCS, which in turn increased viscosity. The fourth solution exhibited the highest viscosity because it had the highest ratio of C_8H_{10} to PCS, whereas the third solution exhibited the lowest viscosity because it had the lowest ratio of C_8H_{10} to PCS.

As depicted in Fig. 8, the solution concentration decreased with the increasing shear rate; viscosity remained constant when the shear rate reached 100 (1/s). This indicated that the PCS solutions were a type of pseudoplastic fluid among non-Newtonian fluids. A non-Newtonian fluid features high viscosity in a quiescent condition, whereas once it begins to flow, the viscosity drops instantly until it reaches a constant level.

PCS is a type of polymer. When PCS solutions were in a quiescent condition, the solutes became aggregated; therefore, the solution exhibited greater viscosity and seemed denser. However, when the shear rate was increased progressively, the solutes within the solutions began to flow and extend instead of aggregating; this led to shear thinning. When the shear rate reached a specific level, the solutes in the solution became completely extended, and the viscosity no longer decreased with increasing shear rate.

3.1.3 Measurement of contact angles of different solution formulas

The contact angle of a solution is one of the factors that affect electrospinning. The degree of surface tension determines whether the solution is able to form a hemispherical droplet at the tip of a spinning tube, in addition to affecting the success of the electrospinning process. A corrosion-resistant plate was employed as the base plate in this experiment to simulate a corrosion-resistant spinning tube. The measurement results are displayed in Fig. 9.

The result indicated that the viscosity increased with increasing contact angle width. The contact angles of the four solutions were all >90°. In general, the contact angle of a solution should be wider than 90° to garner sufficient cohesion to form a hemispherical droplet at the tip of the spinning tube. Under the effect of an electric field, a hemispherical droplet can easily form a Taylor cone and therefore a stable electrospinning jet.

3.2 PCS solution spinnability and fiber analysis

3.2.1 Comparison of the spinnability of PCS solutions

Table 4 depicts the characteristics of electrospinning products acquired from the four solutions under various voltages. In this table, the term “droplets” represents the circumstances where droplets could not be stretched into fibers under static electricity but were directly extruded onto the collector. The term “short fibers” denotes the circumstances in which fibers were broken into tiny fragments. The term “fibers and droplets” indicates how some fibers were obtained using the collector but PCS granules were observed within these fibers. Such granules were formed after tiny droplets, which were extruded onto the collector, became dried. The term “long fibers” indicates that a layer of nonwoven fabric was collected, and no granules were observed using unaided vision.

As evident in Table 4, the fourth solution could only produce a small amount of tiny fibers at 20 kV. The reason was that the fourth solution had the highest viscosity; once the solution came into contact with the air, it would block the tip of the spinning tube and impede the spinning process, as depicted in Fig. 10.

The third solution produced droplets only. This was because the solution exhibited the lowest viscosity; therefore, the solution particles aggregated because of the surface tension, becoming unable to be spun, and was spattered onto the collector as droplets.

Only the first and second solutions demonstrated greater spinnability. The two solutions contained higher amounts of DMF, exhibited high polarity, and were easily stretched under an electric field, all of which enabled the generation of fibers. The viscosity of the two solutions was between those of the third and fourth solutions. Droplets were less likely to be observed when the first or second solution was used, which implied that the viscosity of these two solutions was more applicable. Comparing the fibers synthesized using the first and second solutions under 20 kV and 25 kV revealed that the first solution generated long fibers of similar lengths, whereas tiny droplets were observed when the second solution was used. This indicated that the viscosity and surface tension in the first solution were more favorable. By contrast, the viscosity of the second solution was lower, and the surface tension was relatively higher, which led to a sharper and unstable jets during the spinning process and therefore yielded fibers of uneven size.

3.3 Analysis of PCS fiber electron microscopy

Fig. 11 displays the fibers synthesized using the first solution at 10, 15, 20, and 25 kV and under a 1000× magnification with a scanning electron microscope (SEM).

As evident in Fig. 11, the fibers synthesized at 10 kV possessed large diameters of approximately 10 μm; furthermore, droplets with diameters of 20 μm were also observed, which indicated that fibers were of uneven size. Because of the relatively low voltage, the tensile strength was insufficiently strong, which resulted in fibers with relatively large or even diameters. The diameters of the fibers became smaller when the voltage was increased to 15 kV, but droplets were still observed among fibers. On the surface of the droplets, tiny pores emerged because of the evaporation of the solvents. After the solution was extruded and made contact with the air, the outer layer began to solidify. The vapors within the solvent would then have to break through the outer solid layer to evaporate into the air. This resulted in the formation of

surface pores. Additionally, PCS fibers have to be calcinated to become SiC. The pores would further expand under calcination, which affected the mechanical property of the fibers. Accordingly, pore formation should be avoided when synthesizing such fibers.

At 20 kV, the fibers exhibited even size and droplets emerged; the fiber diameter was approximately 1 μm. At 25 kV, no notable morphological differences were observed. However, comparing the fibers generated under 20 kV and 25 kV revealed that the fibers generated under 25 kV were thinner and more compressed. This indicated that the optimal voltage was 25 kV.

Fig. 12 depicts the fibers synthesized using the second solution at 20 kV and 25 kV and viewed under a 1000× magnification with an SEM. The fibers generated at 15 kV had too many droplets; therefore, they were not observable with an SEM.

In Fig. 12, the fibers formed under 20 kV included many droplets, and round droplets and solids were detected among the long fibers, which suggested that during the process of electrospinning, the fibers were extruded onto the collector before the static electricity was able to stretch them out. However, at 25 kV, long fibers were formed with fewer droplets, but spherical extrusions were clearly seen in the image. This was because the viscosity and the surface tension of the solvents were not balanced.

According to the images displayed in Fig. 11 and 12, increasing the voltage increased the fiber length. However, when the voltage was further increased, the influence of voltage on the fiber diameter became smaller, which corresponds to the results of [10]. The viscosity of the first solution was higher and could offset the surface tension; therefore, the resulting fibers were most even in size. Given that this set of process parameters had the best performance, it was applied to subsequent processes to produce SiC fibers.

3.4 Curing process

3.4.1 Oxygen content of cured PCS fibers

The fibers were placed in a high-temperature furnace and heated to 200°C at an incremental rate of 5 °C/minute. Fig. 13 presents a graph based on the energy dispersive spectrometer analysis on the oxygen content with the temperature maintained for 0.25, 0.5, 1.0, and 2.0 h. The oxygen content increased with the temperature maintenance time, but the increased amount became smaller with a longer time. Increasing the oxygen content reduced the strength of the resulting SiC fibers. Accordingly, the fiber oxygen content should not be overly high. Previous scholars [10] concluded that fibers morphology can be maintained during calcination when the fiber oxygen content is kept at approximately 8.0 at%.

3.4.2 FTIR analysis before and after the curing process

Fig. 14 displays the FTIR spectra before and after the PCS curing process. The main apparent differences are the absorption peaks at 1080 cm^{-1} and 3700 cm^{-1}, which correspond to the presence of Si-OH and Si-

O-Si bonds, respectively. These bonds form an SiOx coating with a high melting point to maintain the fiber morphology during calcination.

During the curing process, after PCS was heated to 200°C, the Si-H and Si-C bonds were oxidized to form Si-OH and Si-O-Si bonds. Other side chains, including Si-CH_3, Si-H, and C-H, reacted with one another and released H_2 and CH_4. Thus, the corresponding absorption peaks were weakened. In addition, [6] reported that the C-H stretching vibration at 2900 cm^{-1} was induced by the trace amount of DMF in the fibers.

3.4.3 SEM analysis after the curing process

Fig. 15 depicts the SEM images of the fibers after the curing process. The fibers were even in size, with an approximate diameter of 1 μm. The effect of curing on the fibers nonapparent because the temperature was only sustained for 0.5 h and because the oxygen content was low.

3.5 Fiber calcination

3.5.1 Thermal analysis of the calcination process

Fig. 16 displays the thermal analysis of the calcination process. The rate of temperature increase was 10°C/minute, and the experiment was conducted under a nitrogen flux. The thermogravimetric weight loss was divided into two phases. First, from 400°C to 800°C, the rapid weight loss (up to 40wt%) occurred due to the pyrolysis of the side chains and chemical bonds within the polymer. Second, from 800°C to 1100 °C, the weight loss converged (<2wt%) because of the emission of residual C, H, and related compounds. Three peaks were discovered when employing differential scanning calorimetry. The absorption peak at 200°C indicated the melting of PCS in the fibers. From 400°C to 800°C, the absorption peak corresponded to the pyrolysis of the fibers. This indicated that PCS was converted from organic compounds to ceramics in this stage. The absorption peak from 1100°C to 1200°C was speculated to correspond to the energy released by the SiC crystallization process.

3.5.2 X-ray diffraction analysis of the PCS fibers after calcination

The calcination temperature and its sustained time would affect the final SiC crystallization; hence, a small amount of the specimen was first applied to conduct the calcination experiment. An X-ray diffraction (XRD) spectrum analysis was employed to examine whether the crystallization was in a β-crystalline phase. The calcination occurred at an incremental rate of 10°C/min. Fig. 17 presents the XRD spectrum of PCS fibers after calcination. In the spectrum, no significant diffraction peaks were observed with temperature sustained for 1 h at 1100°C, which indicated that the specimen was an amorphous solid. After extending the temperature maintenance time to 3 h at the same temperature, weak peaks began to occur, and they all corresponded to the β-SiC diffraction peaks. This indicated that a β-crystalline phase could not be formed at 1100°C. Even if the temperature retention time was extended to 3 h, crystallization could not occur among the molecules. The specimen calcinated at 1200°C with temperature sustained for 2 h displayed notable diffraction peaks when the angle 2θ was 36°, 42°, 60°,

and 72°, and the XRD curve corresponds to that recorded in the JCPDS file No.29-1129. This verified that the resulting product was β-SiC.

3.5.3 SEM analysis of SiC fibers

The fibers were inserted into a tubular furnace after the curing process and were heated to 1200°C at an increasing rate of 10°C /min in a nitrogen flux for 2 h, which pyrolyzed PCS into SiC. The diameter of the fibers was 0.8 μm, as presented in Fig. 18. The fibers were long, even, complete, and without pores.

3.5.4 Energy-dispersive X-ray spectroscopy analysis of SiC fibers

SiC fibers were subjected to energy-dispersive X-ray spectroscopy (EDS) analysis, as shown in Fig. 19. The percent composition of the SiC fibers was 57.3% C, 33.5% Si, and 9.2% O. Oxygen was introduced during the curing process to form a protective coating. The excessive amount of carbon was derived from the polymer side chain, a common byproduct in the Si-H compound pyrolysis process.

3.5.5 Transmission electron microscope analysis of SiC fibers

The selected area diffraction and the crystal lattice of SiC fibers are displayed in Fig. 20 and 21, respectively. In Fig. 20, comparing the SiC selected area diffraction results to those in [11] revealed that the crystal phase was a simple cubic structure and the Miller index was 111, which accords with the relevant literature. The result of the selected area diffraction was verified to be β-SiC fibers because the β crystal phase was in a simple cubic structure. Previous scholars [12] indicated that the crystal lattice spacing was approximately 0.26 nm. The result in Fig. 21 matches the result of that study.

4 Conclusion

(1) When PCS was refined at 200°C in a nitrogen flux for 1 h, its weight and polydispersity declined, but its molecular weight and the degree of polymerization increased, which strengthened the quality of the precursors.

(2) The volume ratio of the C_8H_{10} solvent and DMF was 70:30. The solvent containing 1.0 g/ml of PCS exhibited the optimal spinnability and enabled the synthesis of continuous fibers with a approximate diameter of 1.0 μm under 25 kV.

(3) PCS fibers cured at 200°C in the air for 0.25 h formed the Si-O-Si bond, which protected the surface of the fibers and prevented the fibers from melting under calcination.

(4) Cured PCS fibers formed β-SiC crystalline fibers under calcination at a sustained temperature in a nitrogen flux. The fibers exhibited an approximate diameter of 0.8 μm and, featured smooth surface, was even in size.

References

1. Yajima S, Hasegawa Y, Hayaski J, *et al.* Synthesis of continuous silicon carbide fibre with high tensile strength and high Young's modulus. Part I: Synthesis of polycarbosilane as precursor. *J Mater Sci* 1978, **13**: 2569–2576.
2. Hasegawa Y, Iimura M, Yajima S, Synthesis of continuous silicon carbide fibre. Part 2 Conversion of polycarbosilane fibre into silicon carbide fibres. *J Mater Sci* 1980, **15**: 720–728.
3. Yajima S, Hasegawa Y, Okamura K, *et al.* Development of high tensile strength silicon carbide fibre using an organosilicon polymer precursor. *Nature* 1978, **273**: 525–527.
4. Wu YB, Zhang GJ, Liu CJ, *et al.* Research Development of Curing Treatment of Polycarbosilane to Prepare Continuous SiC Fibre. *Mater Rev* 2006, **20**: 80–87.
5. Hasegawa Y, Synthesis of continuous silicon carbide fibre. Part 6 Pyrolysis process of cured polycarbosilane fibre and structure of SiC fibre. *J Mater Sci* 1989, **24**: 1177–1190.
6. Setiawan J, Fatimah S, Poertadji S, *et al.* Characterization of Electrospinning Polycarbosilane Fiber with the Concentration of N,N-Dimethylformamide 22%, 24%, 26%, 28% and 30%. *Appl Mech Mater* 2014, **621**: 44–49.
7. Yang DX, Xiao P, Zhao XF, *et al.* Processing Continuous Submicro/Nano SiC Fibers by Electrospinning. *Chi Surf Eng* 2010, **23**: 39–44.
8. Yuan Y. Synthesis of silicon carbide fibers from polycarbosilane by electrospnning method. Master Thesis. South Carolina, America: Clemson University, 2014.
9. Kim YH, Shin DG, Kim HR, *et al.* Preparation of polycarbosilane using a catalytic process and its practical uses. *Key Eng Mater* 2005, **287**: 108–111.
10. He SW. Analysis and verification on influencing factors of nanofiber morphology by electrospinning. Ph.D. Thesis. Shanghai, China: Donghua University, 2011.
11. Liu JM, Chen WY, Hwang J, *et al.* Growth of 3C–SiC on Si(111) using the four-step non-cooling process. *Thin Solid Films* 2010, **518**: 5700–5703.
12. Xu QF, Deng Z, Sun QY, *et al.* Electrically conducting graphene/SiC(111) composite coatings by laser chemical vapor deposition. *Carbon* 2018, **139**: 76–84.

Tables

Table 1 Experimental parameters of solution formation

DMF/(DMF+xylene) % (v/v)	PCS content (g/ml solvent)
0	1.0
10	1.1
20	1.2
30	1.3
40	1.4
	1.5

Note: Cross-match was performed using 30 experiments.

Table 2 Parameters defined in the electrospinning experiment

Voltage (kV)	Extrusion rate (ml/h)	Spinning distance (cm)
10	1.0	15
15		
20		
25		

Note: A total of four experiments were performed.

Table 3 Experimental parameters of the curing process

Rate of temperature increase (°C/min)	Temperature (°C)	Duration of temperature maintenance (h)
5	200	0.25
		0.5
		1.0
		1.5
		2.0

Note: A total of five experiments were performed.

Table 4 Electrospinning products of PCS solutions

Solution Voltage	(1)	(2)	(3)	(4)
10 kV	fibers with droplets	droplets	droplets	droplets
15 kV	fibers with droplets	fibers with droplets	droplets	droplets
20 kV	long fibers	long fibers with tiny droplets	droplets	short fibers
25 kV	long fibers	long fibers with tiny droplets	droplets	short fibers

Figures

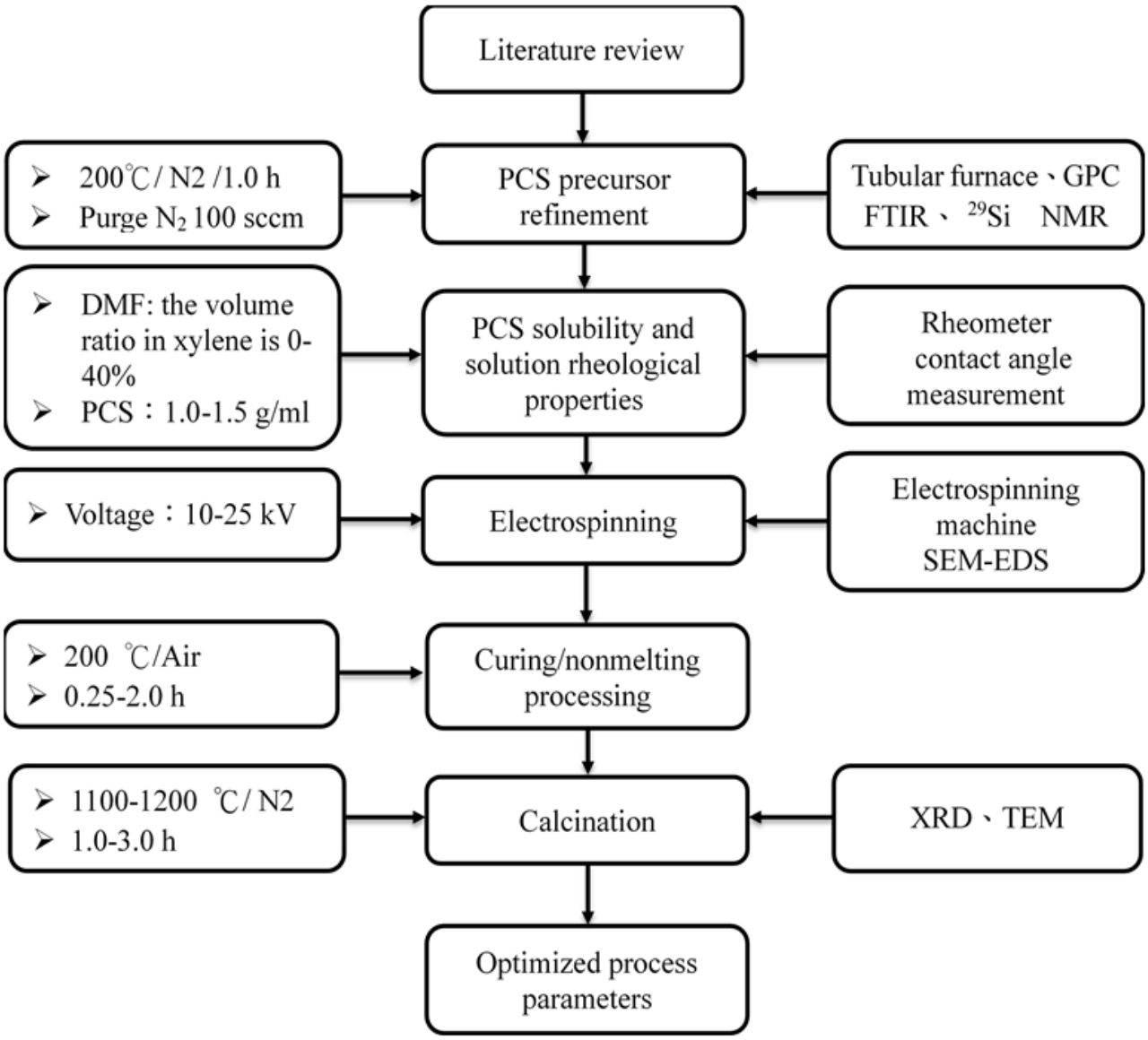

Figure 1

Experimental procedure

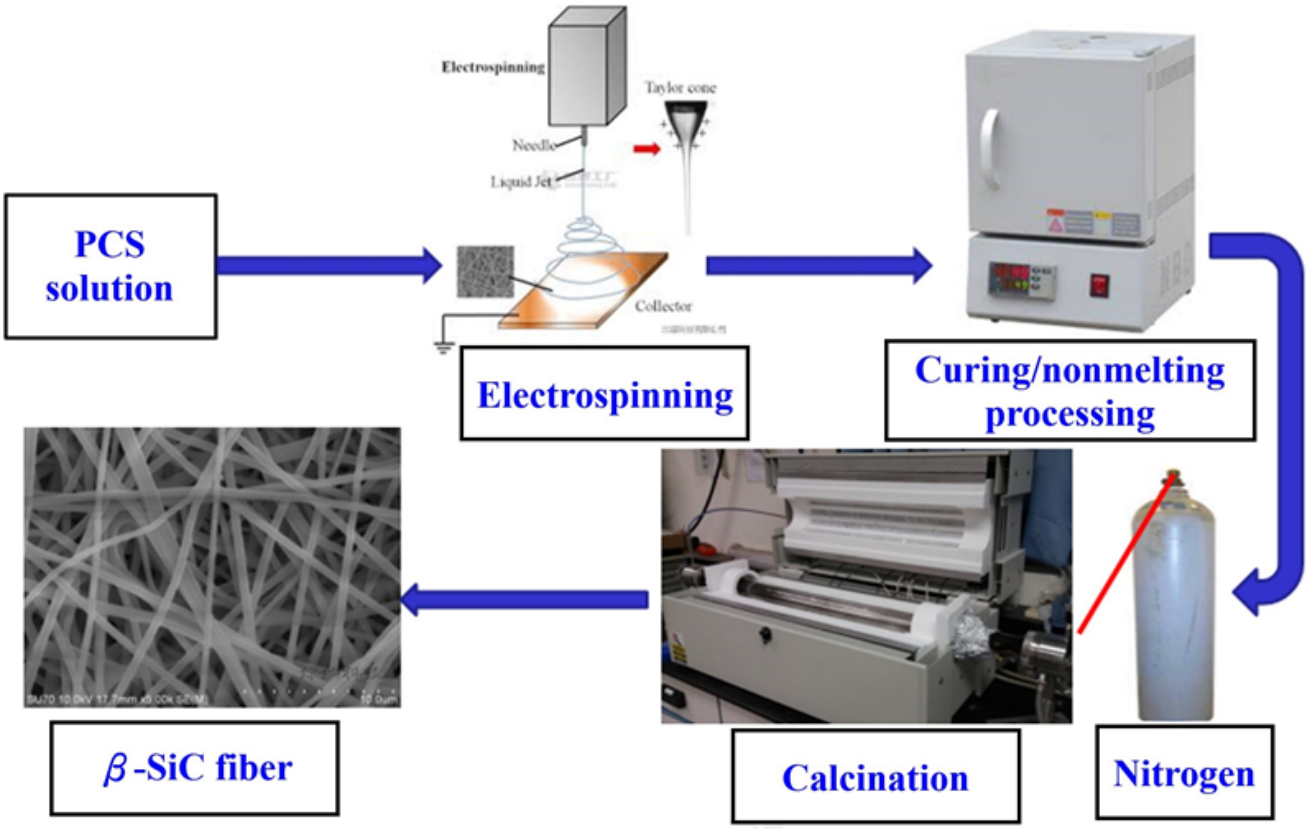

Figure 2

Diagram of β-SiC fiber production

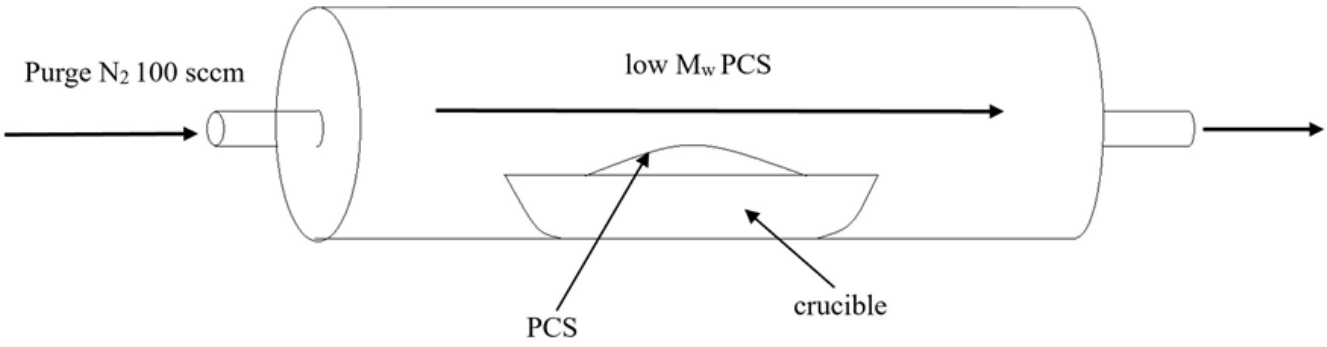

Figure 3

Configuration of precursor refinement

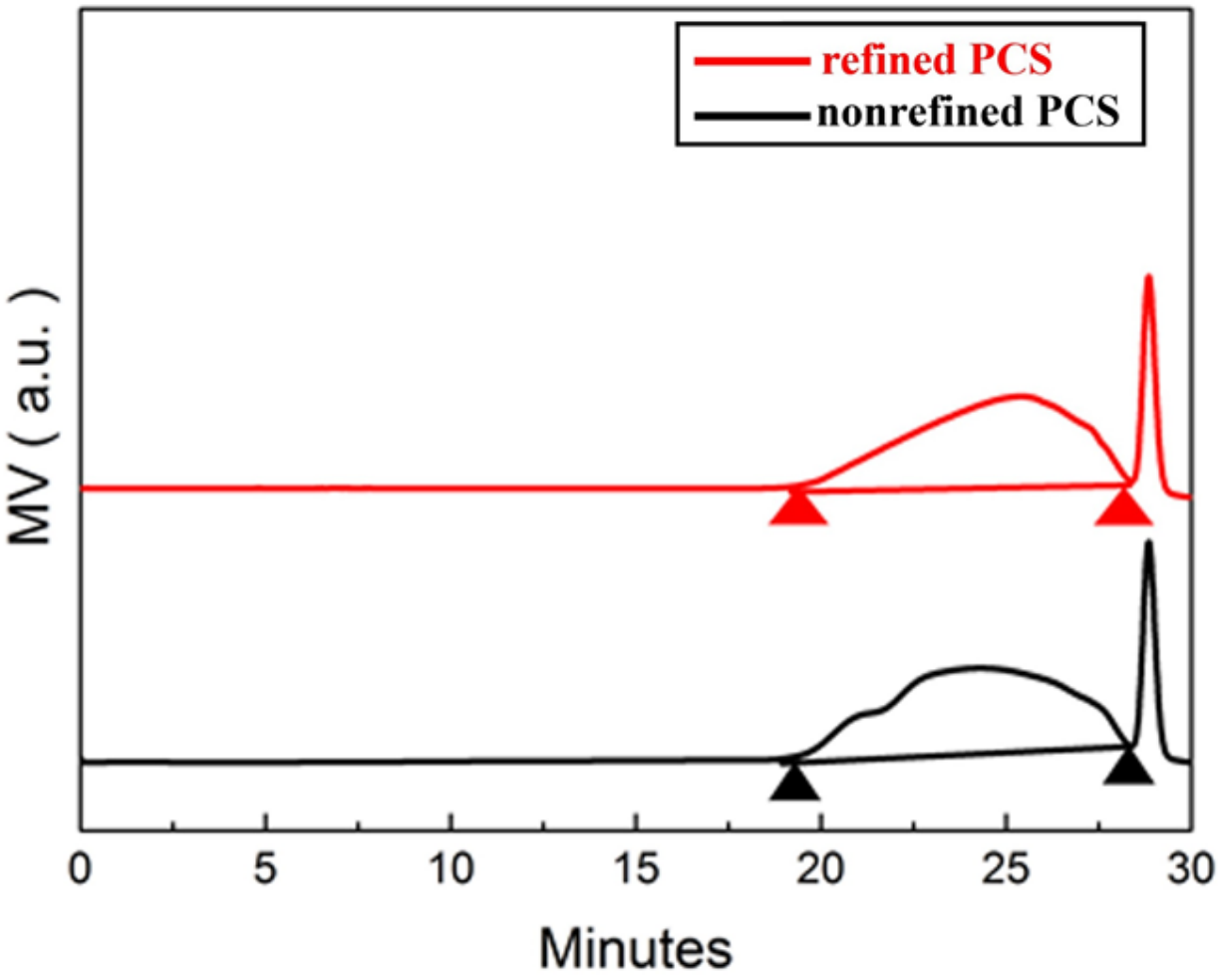

Figure 4

Gel permeation chromatography spectrum before and after refinement

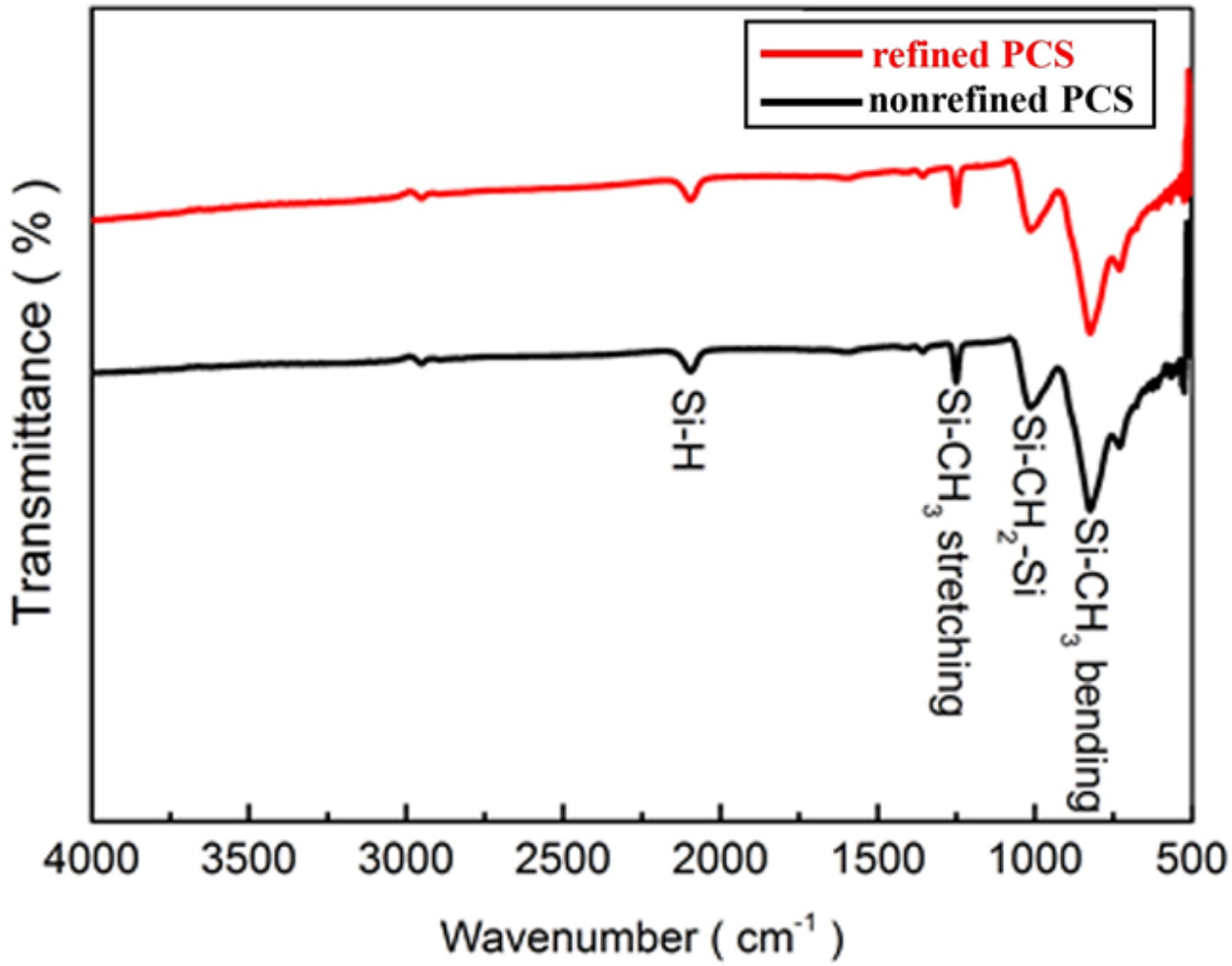

Figure 5

FTIR spectra of PCS precursors before and after refinement

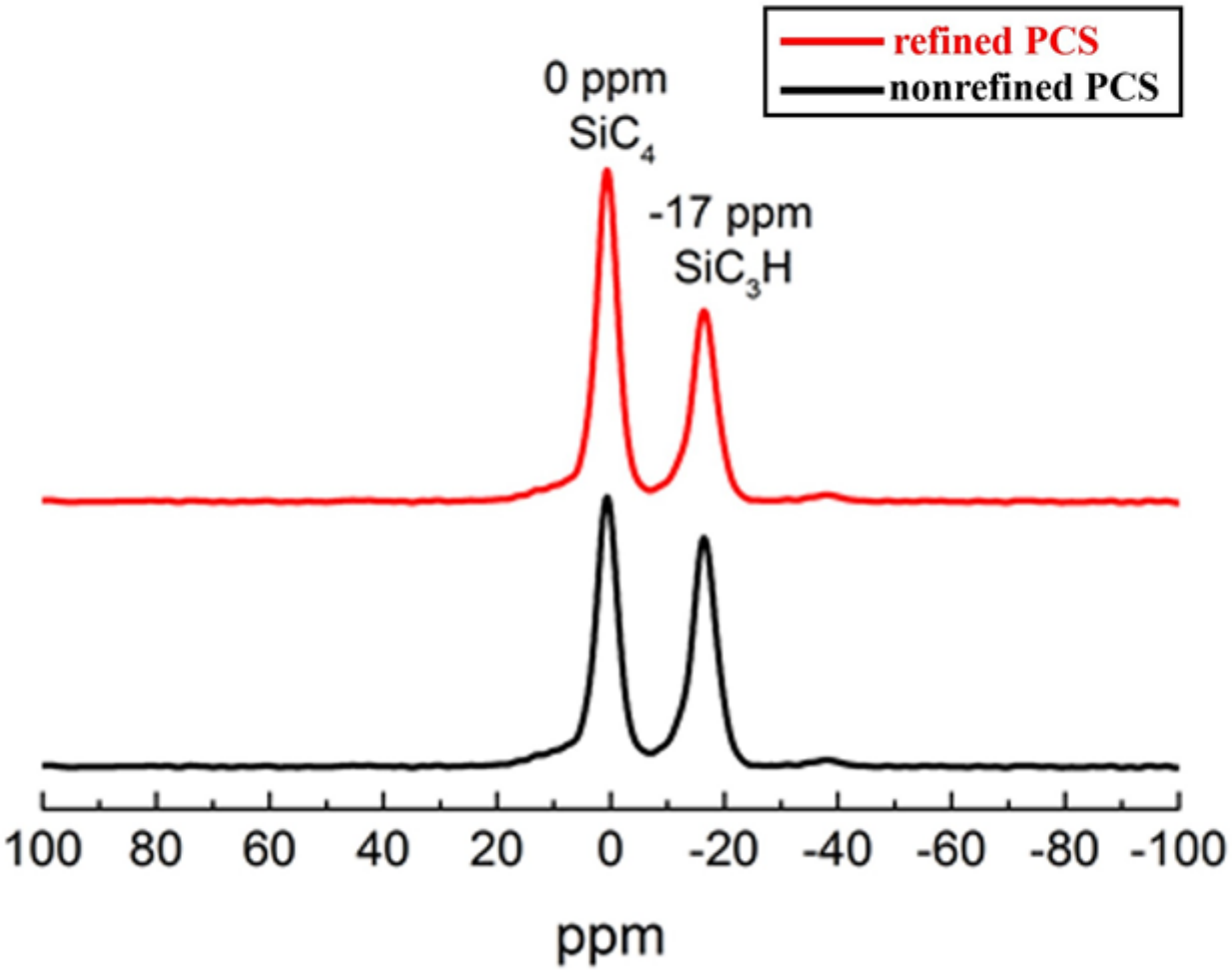

Figure 6

29Si NMR spectra of PCS precursors before and after refinement

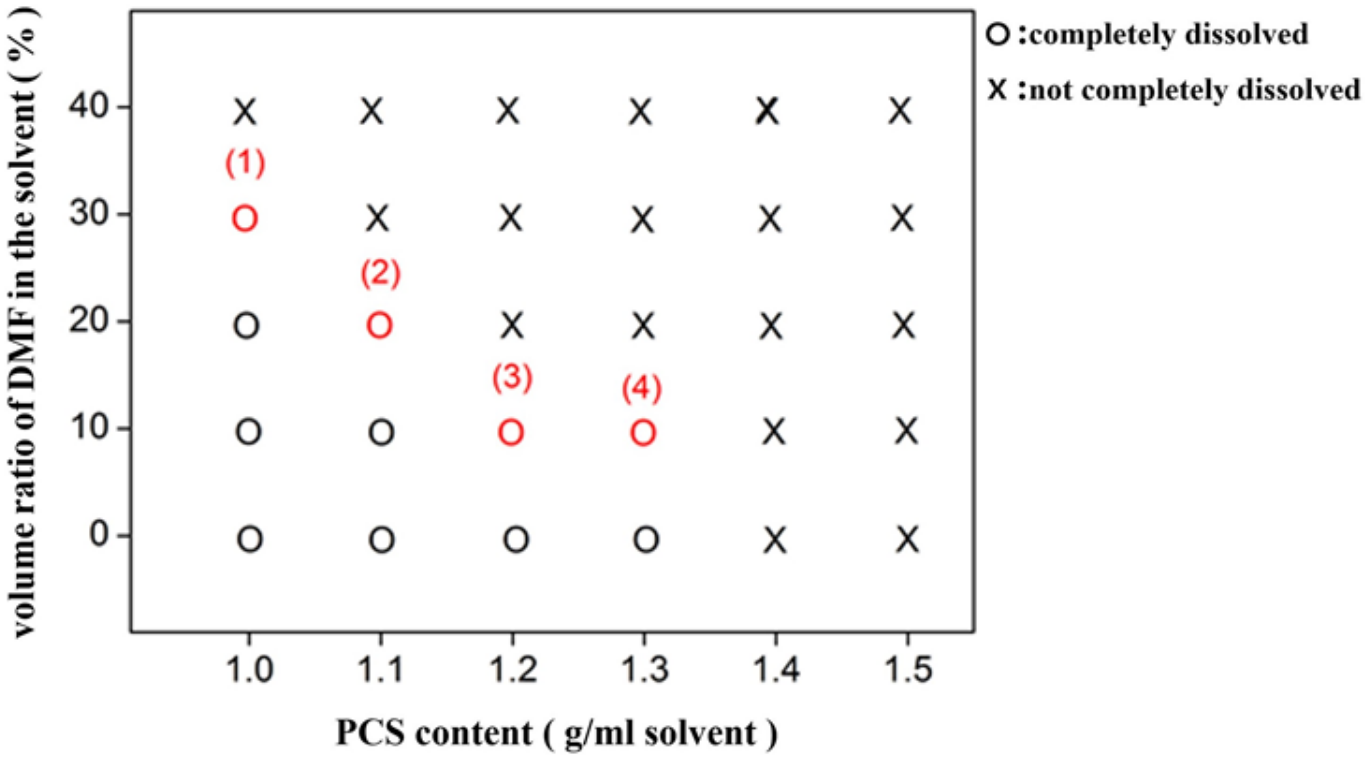

Figure 7

Solubility of PCS in each solution

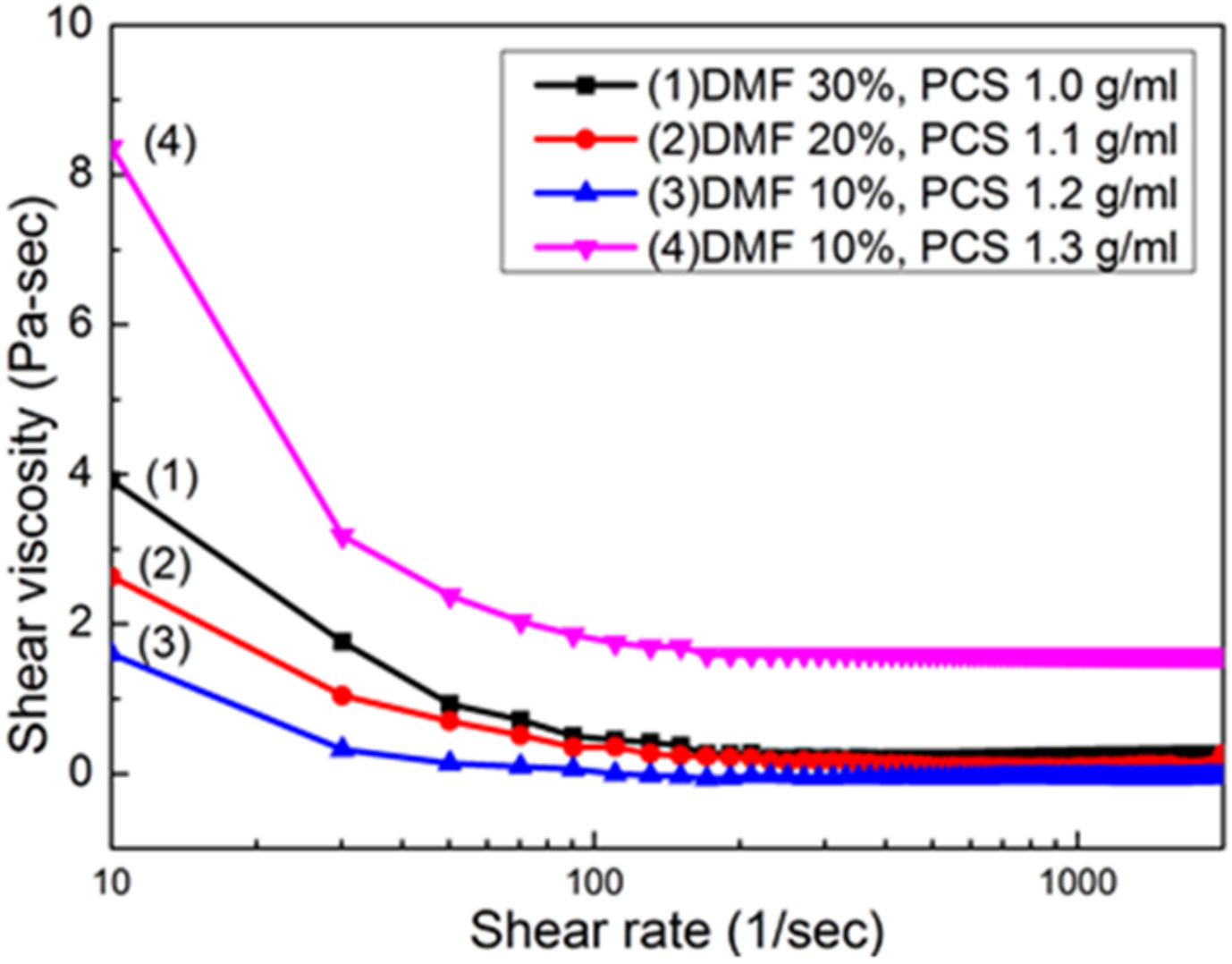

Figure 8

Viscosity of each solution formula

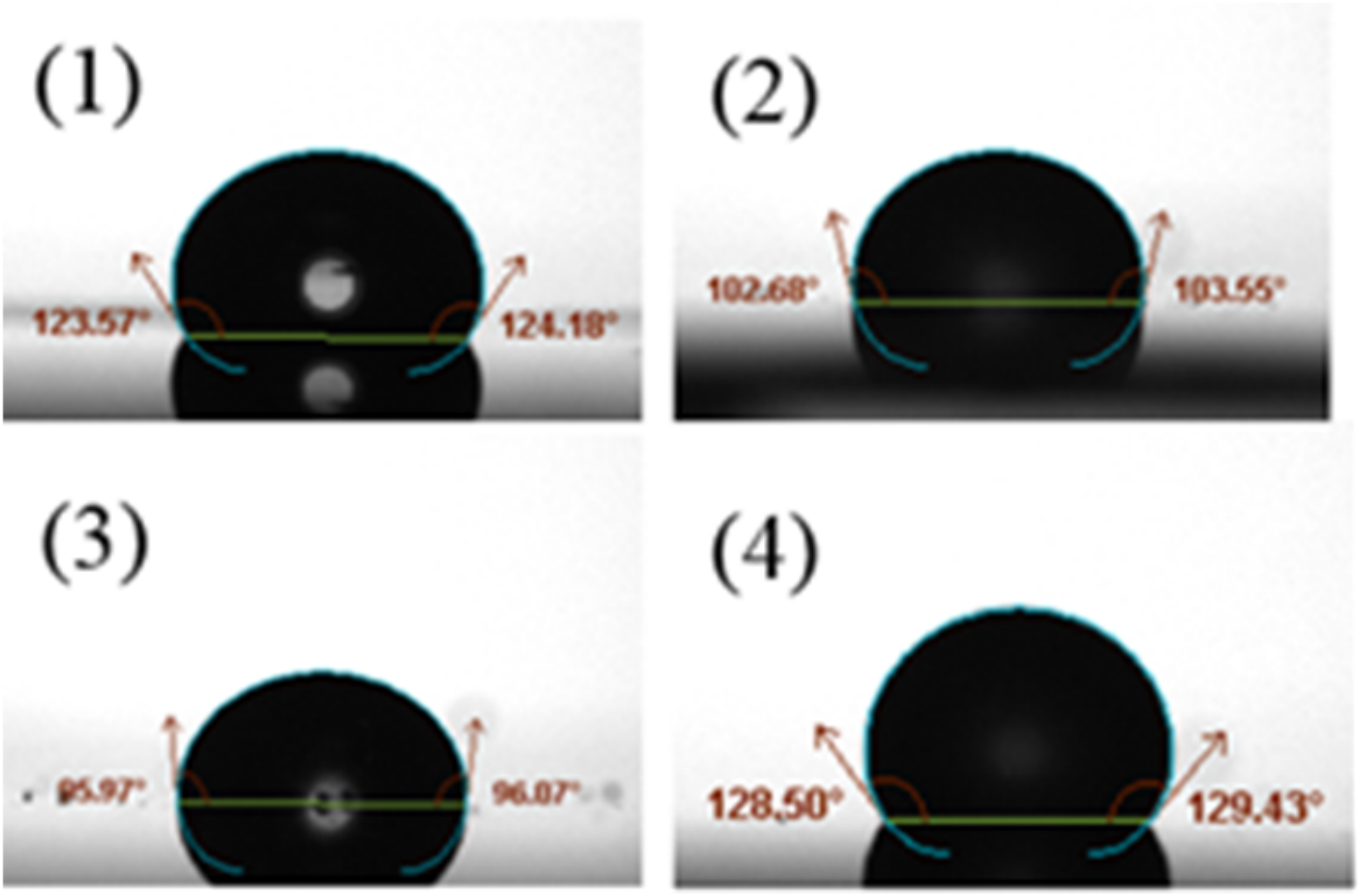

Figure 9

Contact angle measurement of solution formulas

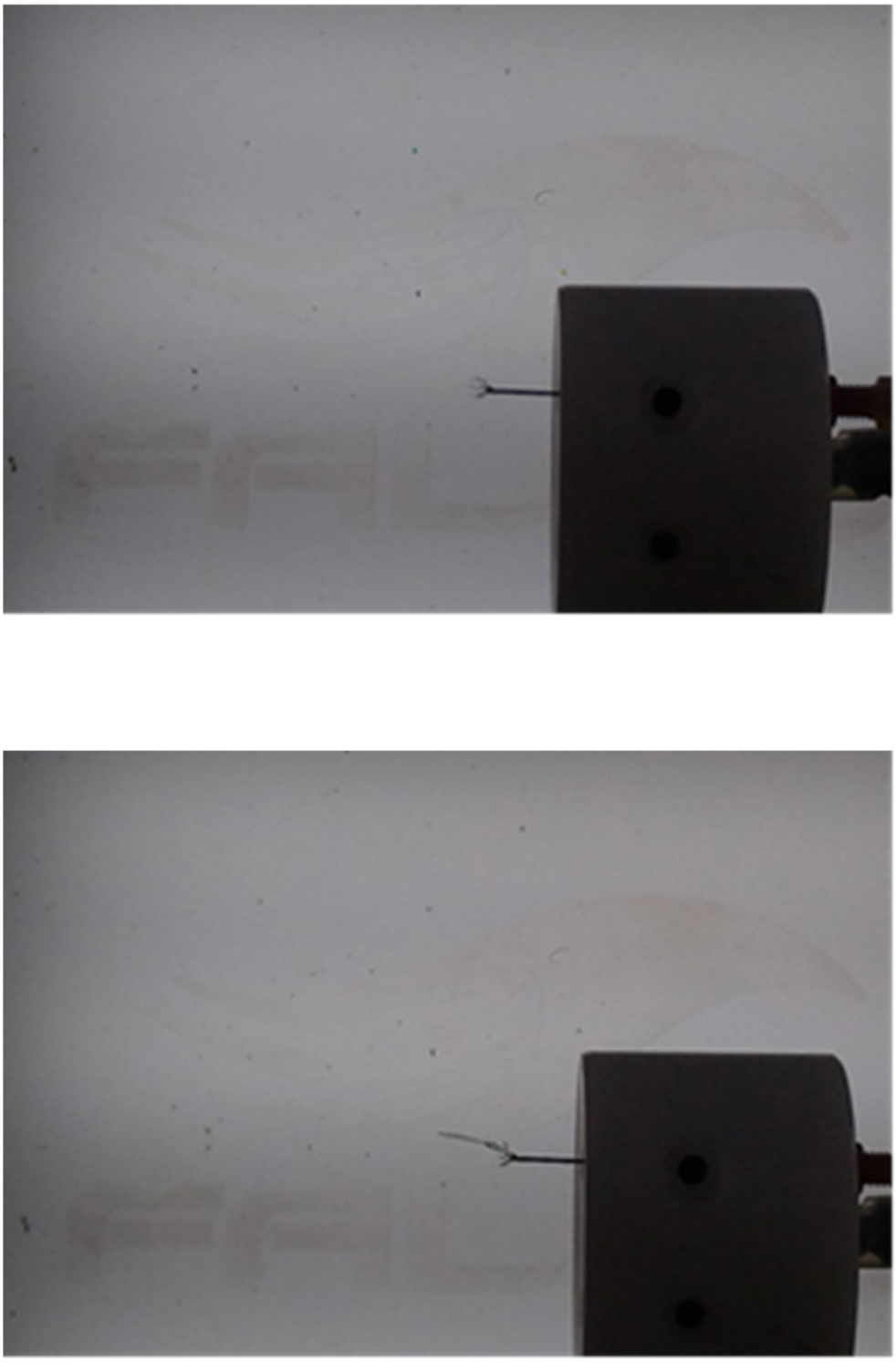

Figure 10

Highly viscous solution blocking the tip of the spinning tube

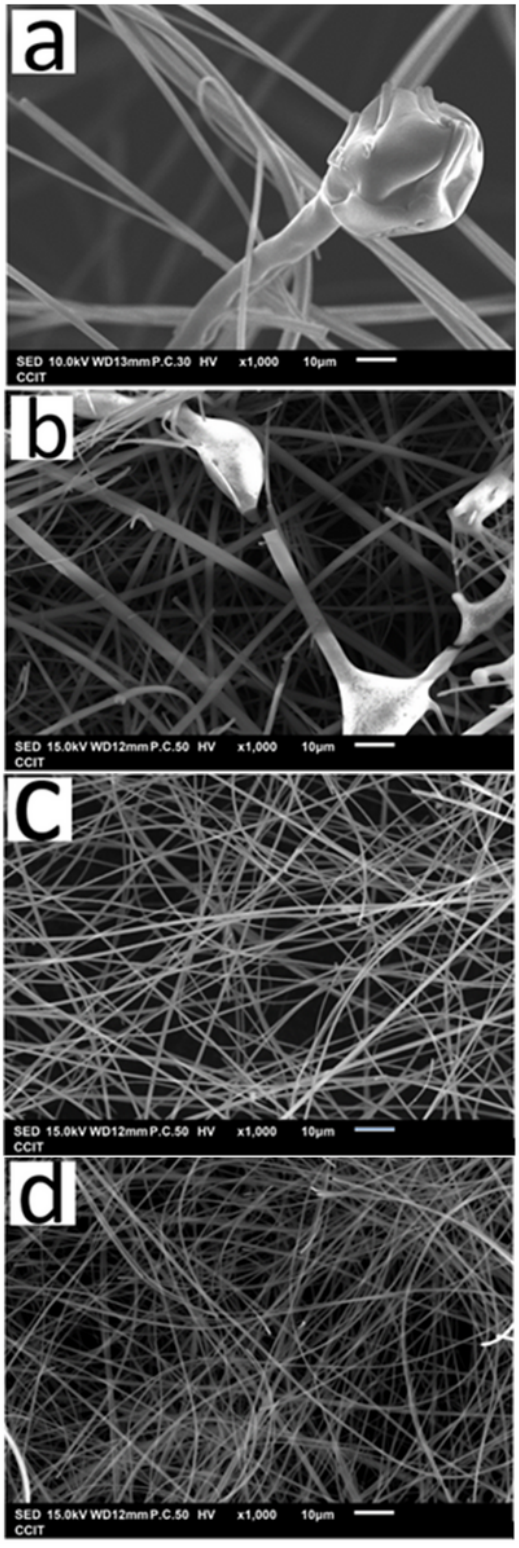

Figure 11

SEM images of the fibers produced using the first solution (a)10 kV (b)15 kV (c)20 kV (d)25 kV

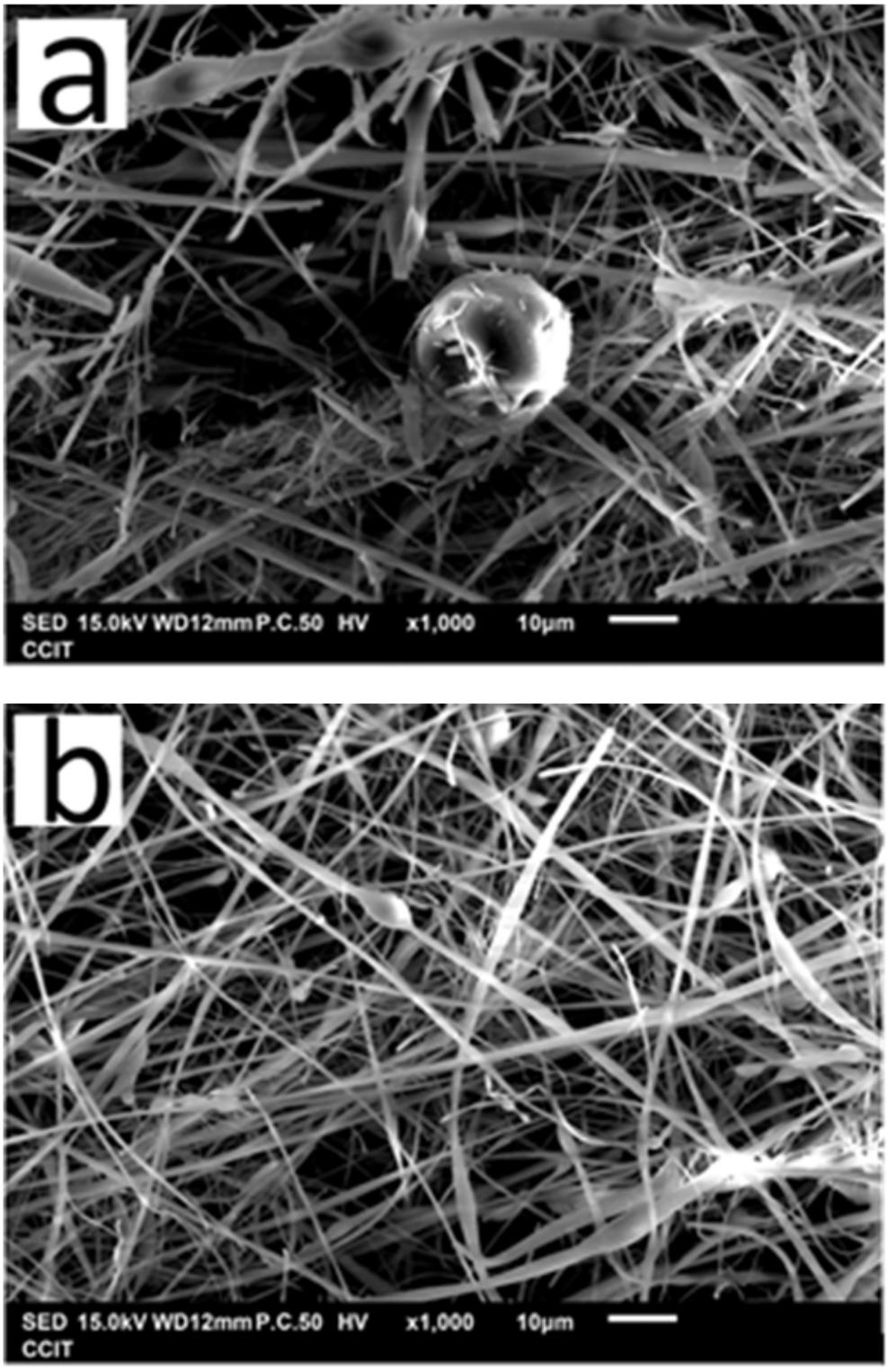

Figure 12

SEM images of the fibers produced using the second solution (a)20 kV (b)25 kV

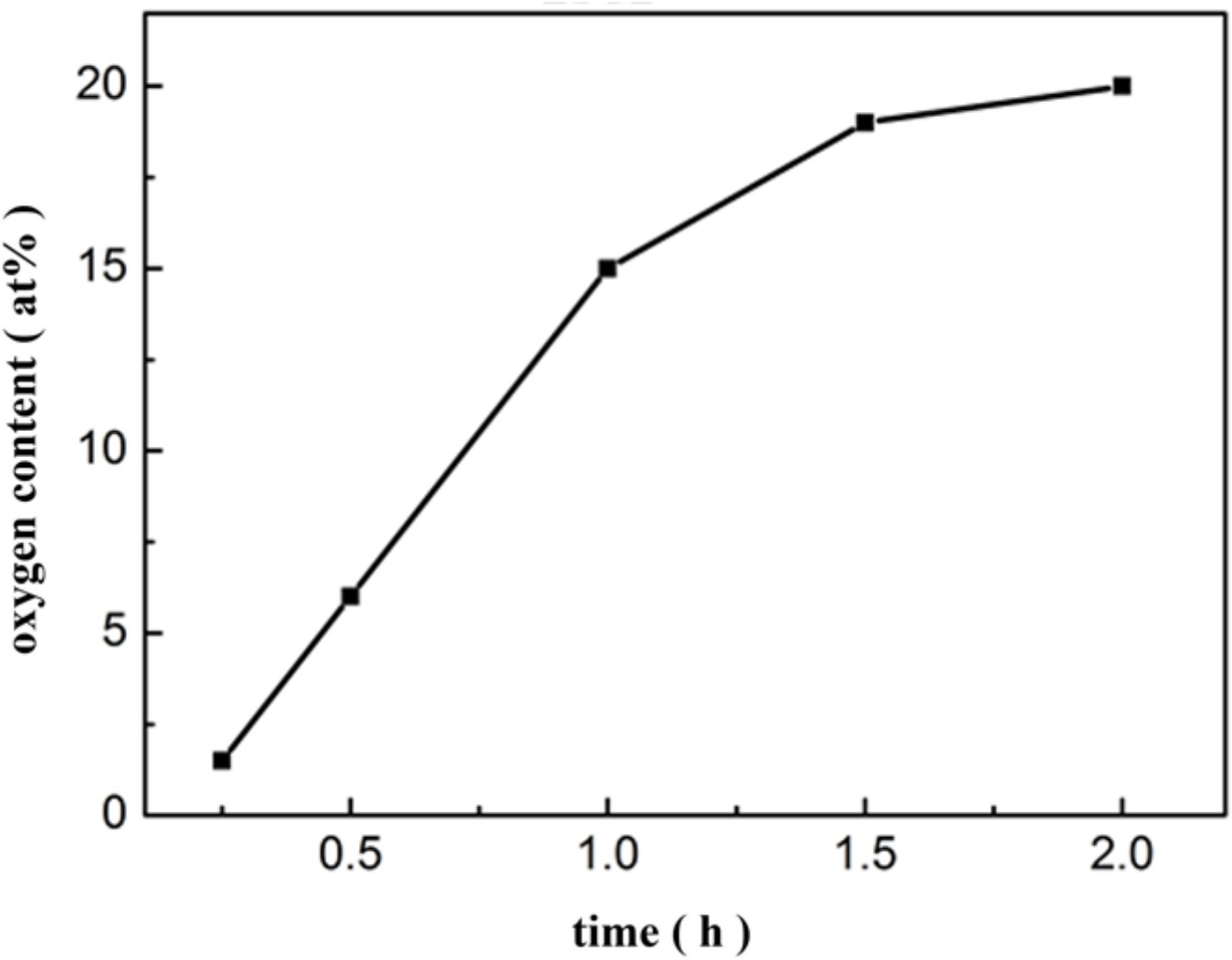

Figure 13

Analysis of temperature maintenance time and oxygen content

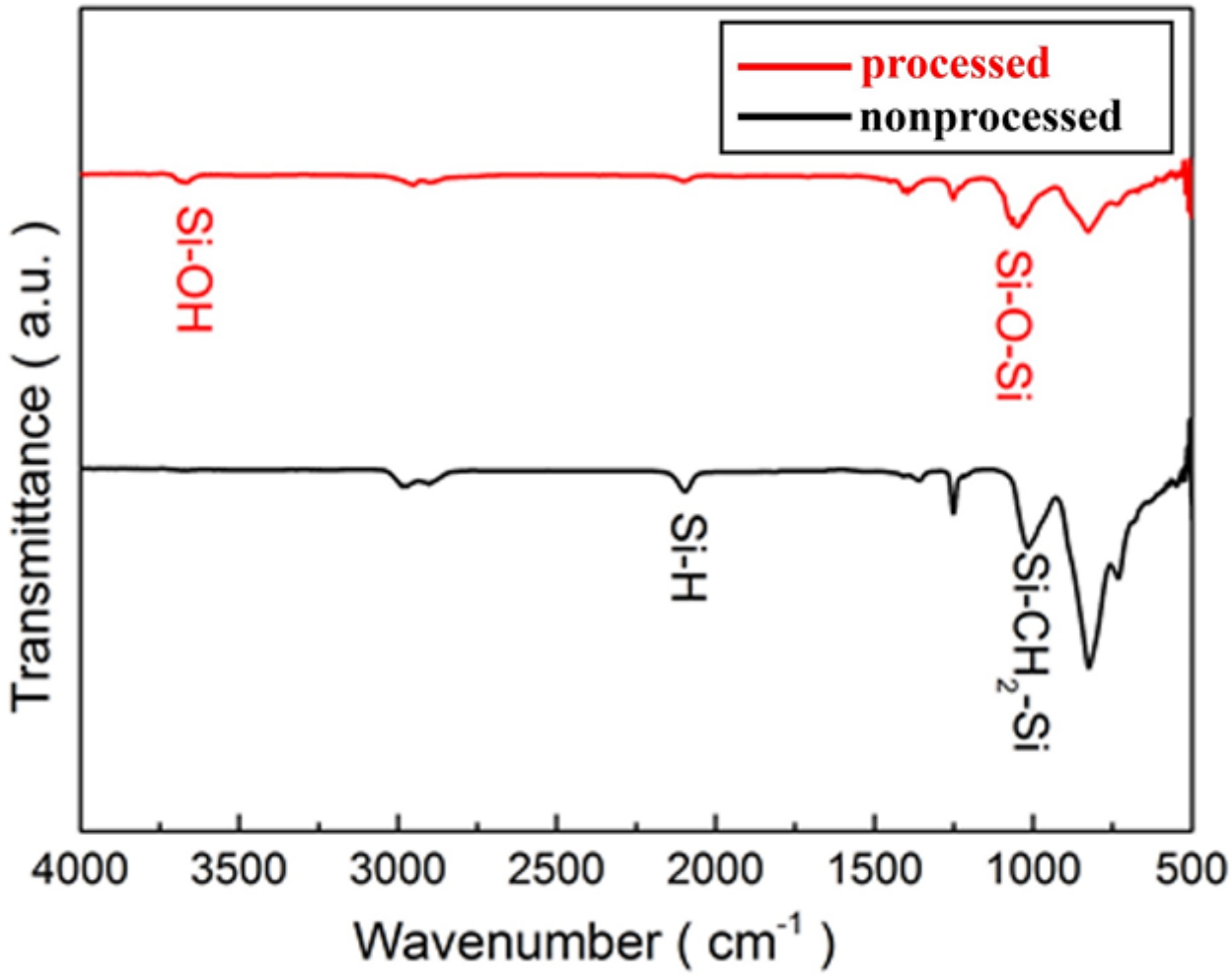

Figure 14

FTIR analysis of processed PCS fibers

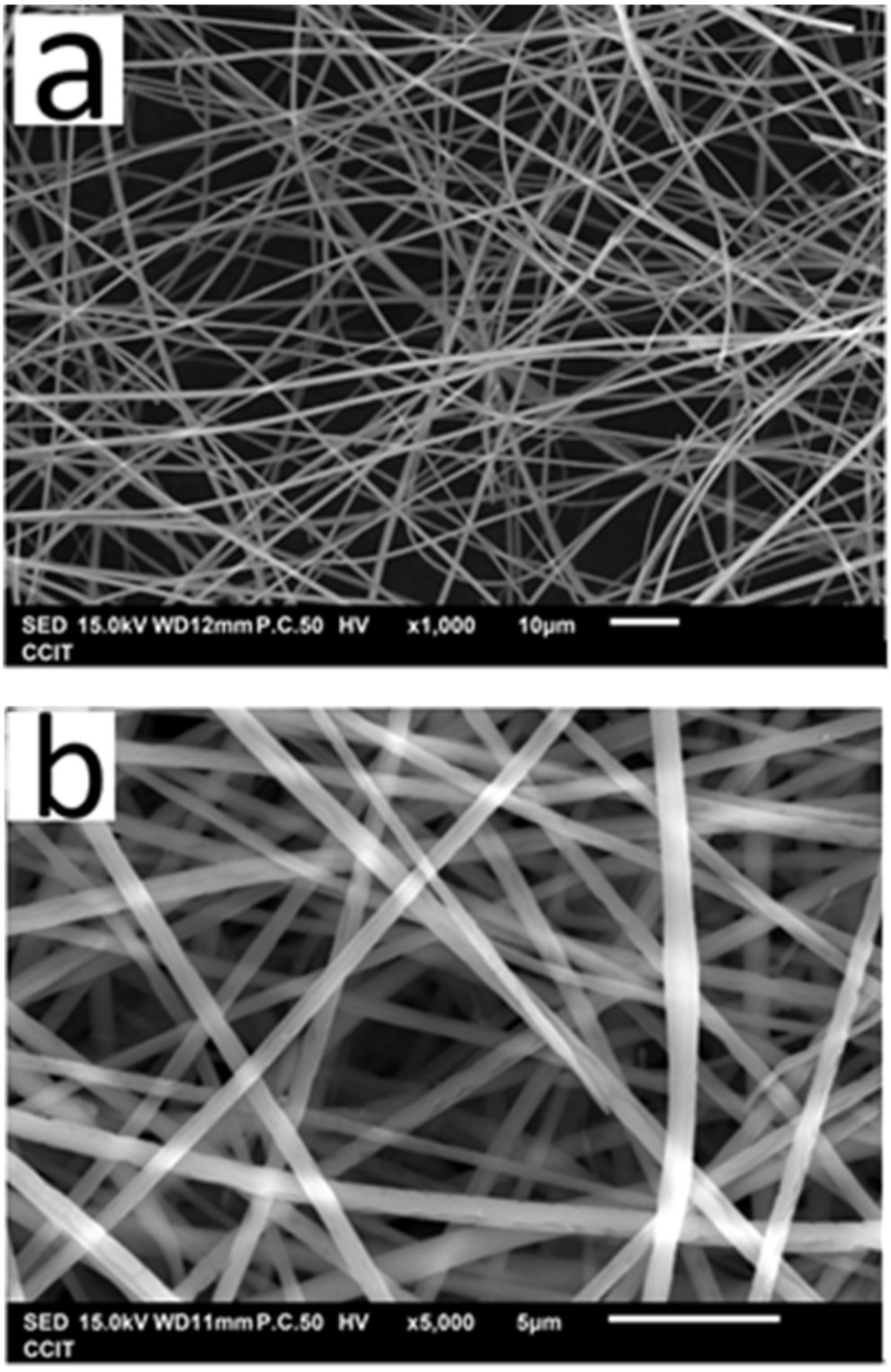

Figure 15

SEM images after the curing process (a)1000× magnification (b)5000× magnification

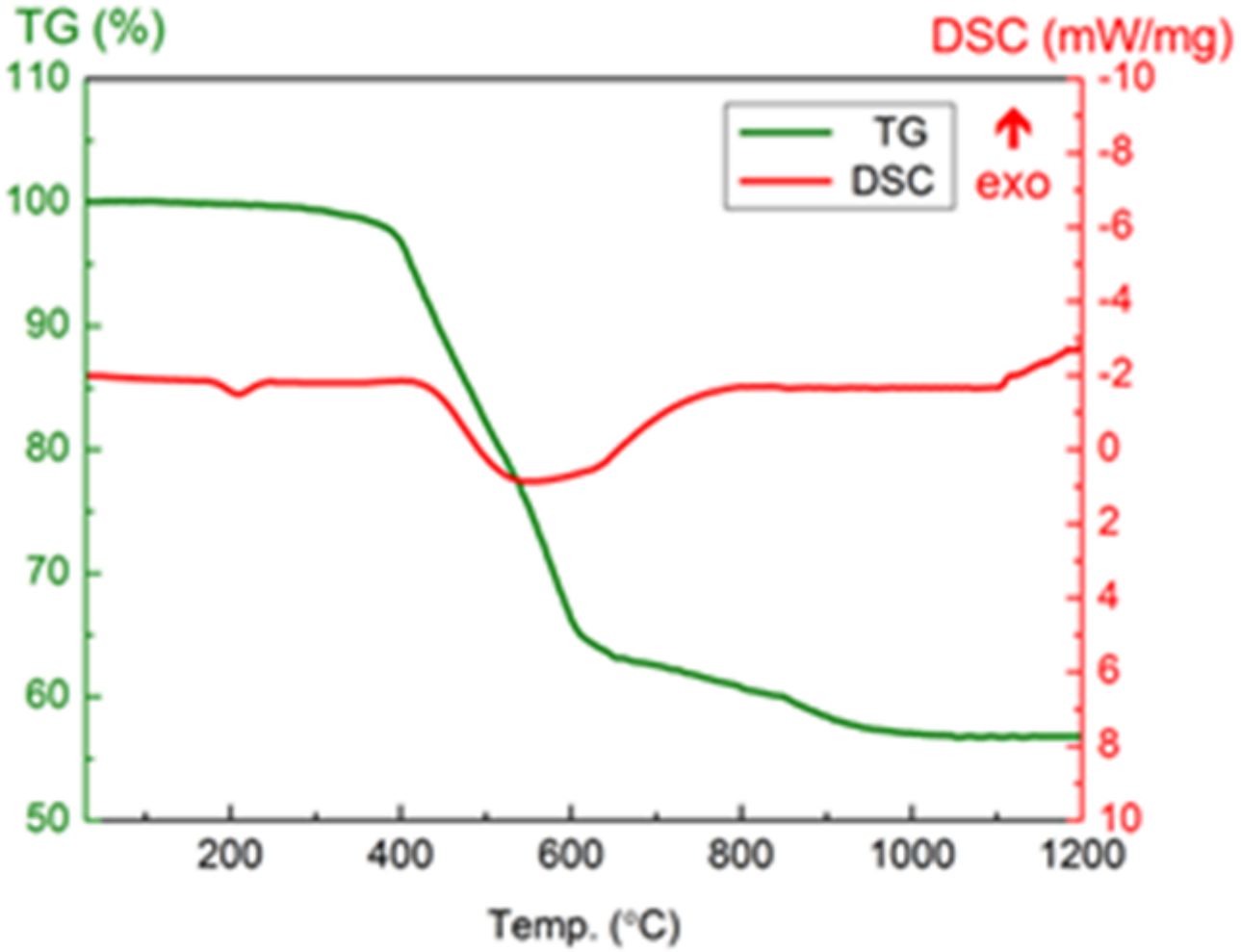

Figure 16

Thermal analysis of the calcination process

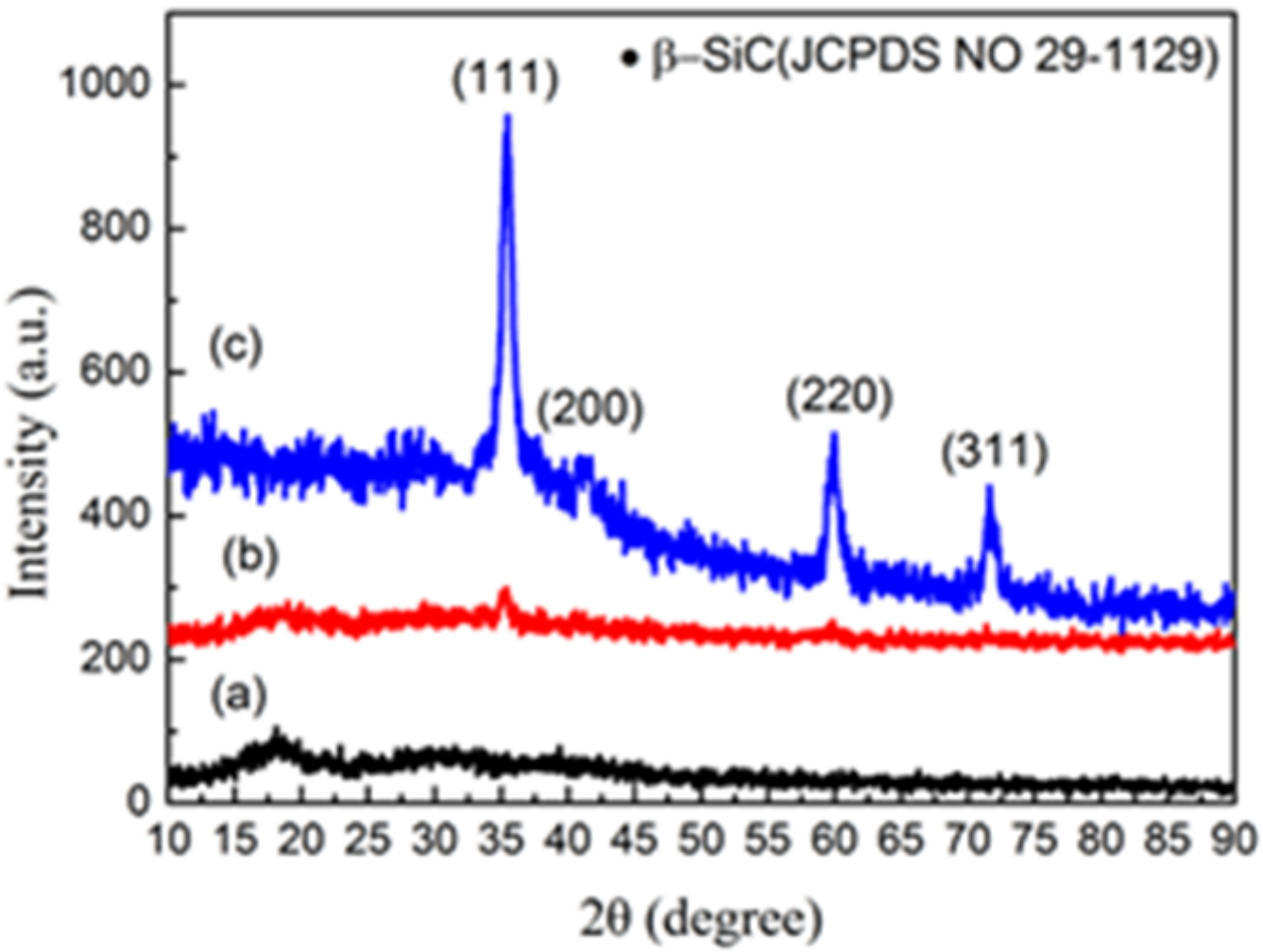

Figure 17

XRD analysis of calcined fibers (a)1100°C, 1 h temperature retention (b)1100°C, 3 h temperature retention (c)1200°C, 2 h temperature retention

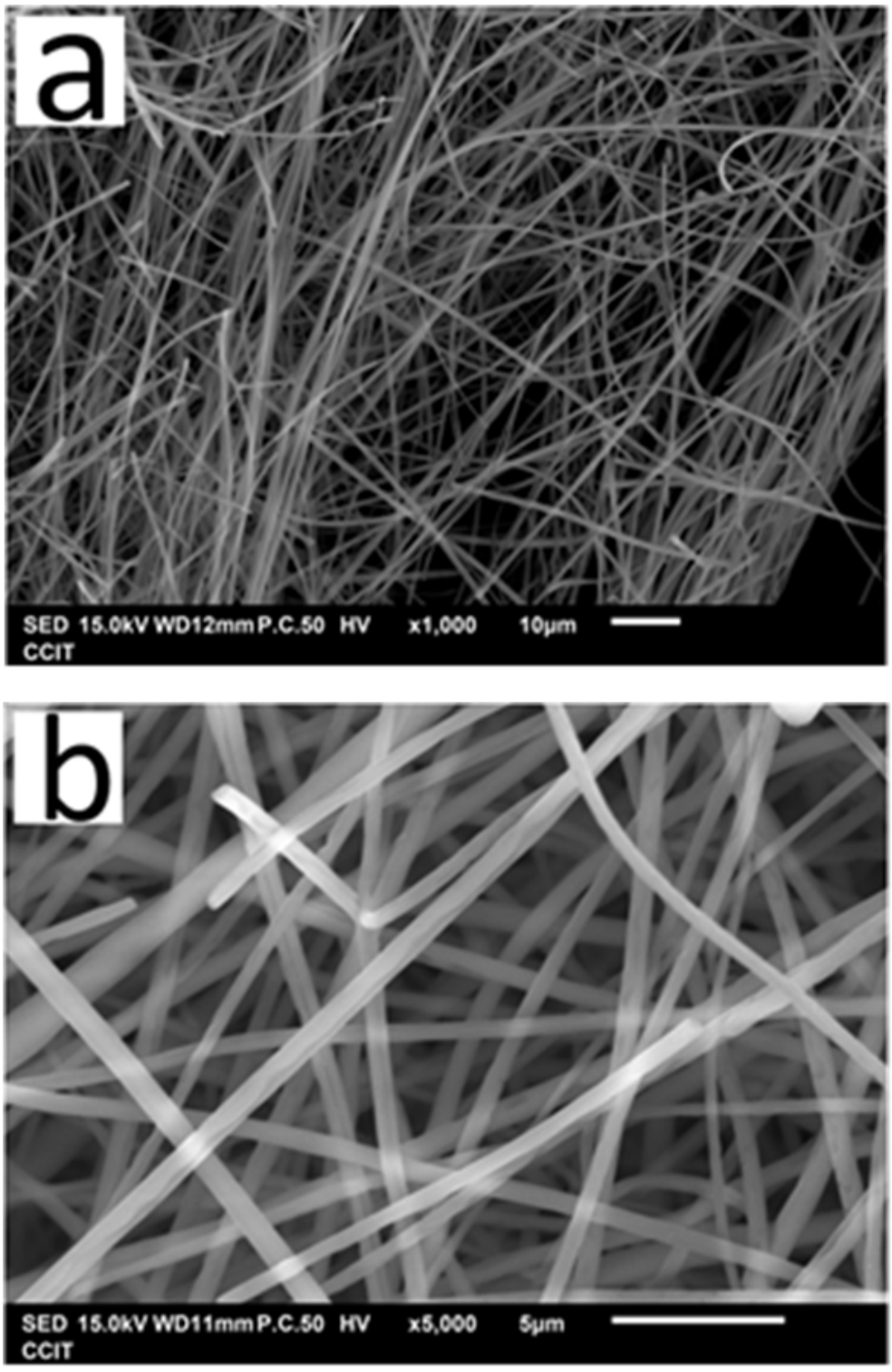

Figure 18

SEM images of fibers after calcination

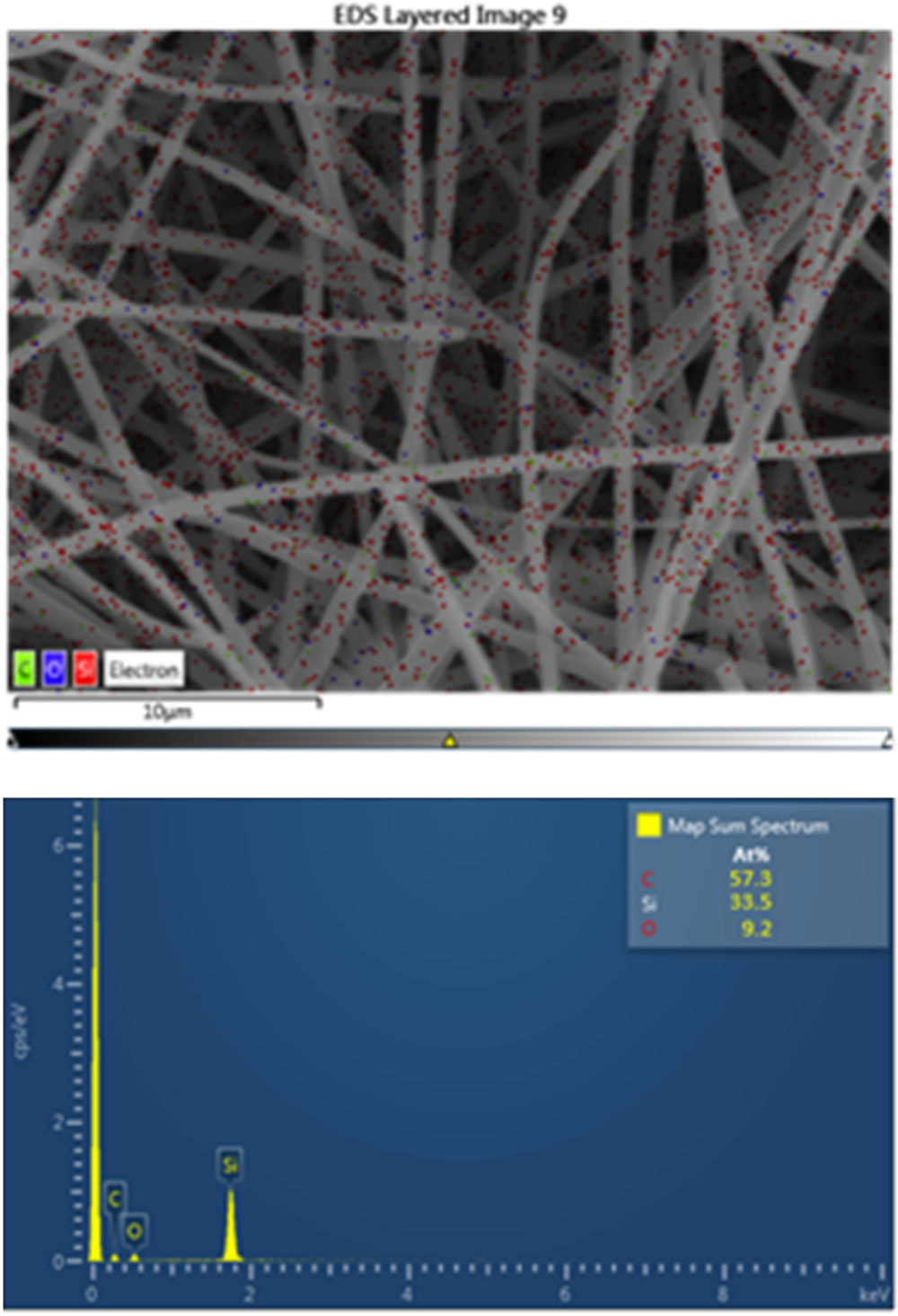

Figure 19

EDS analysis of SiC

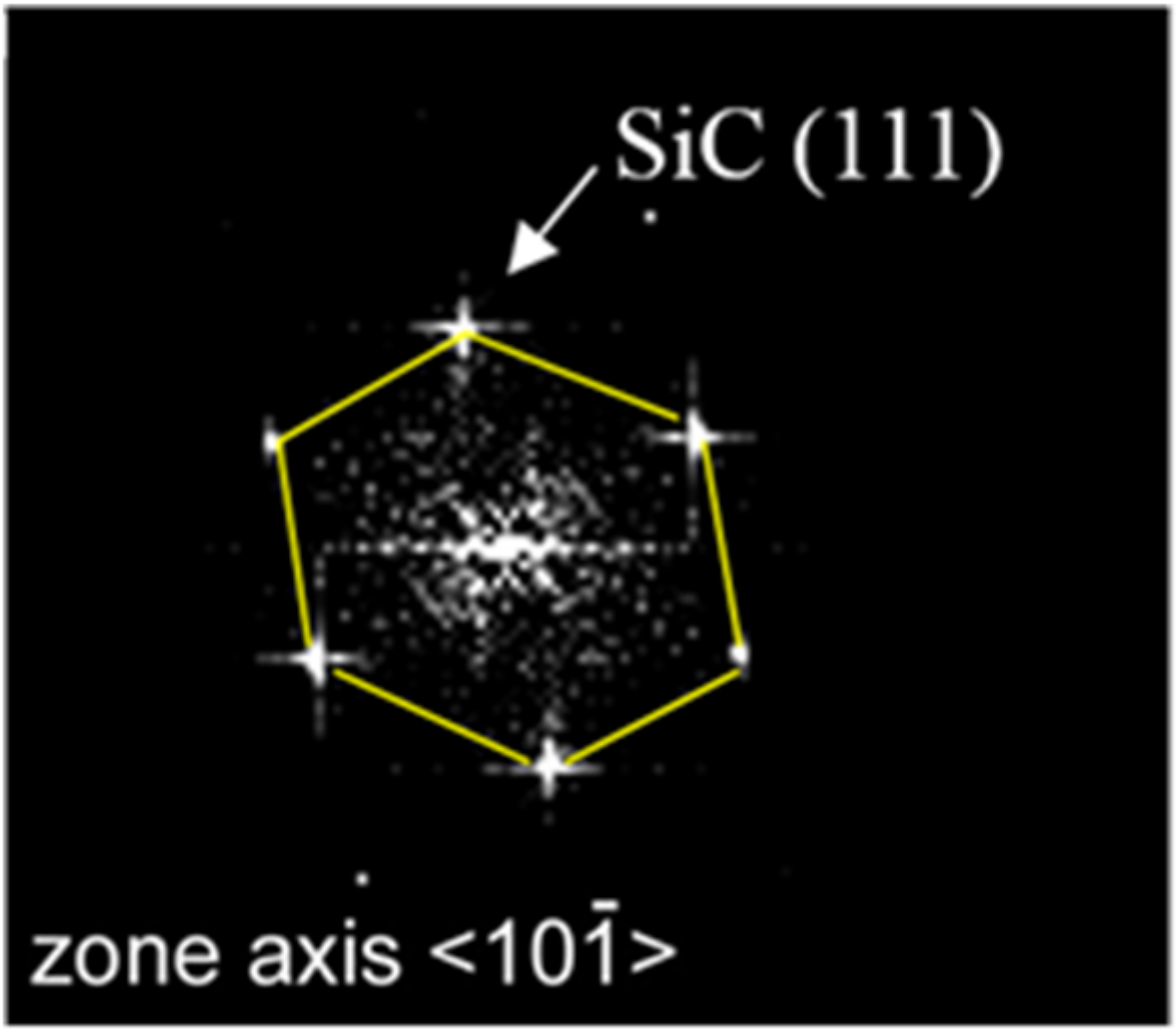

Figure 20

Selected area diffraction spectrum of SiC fibers

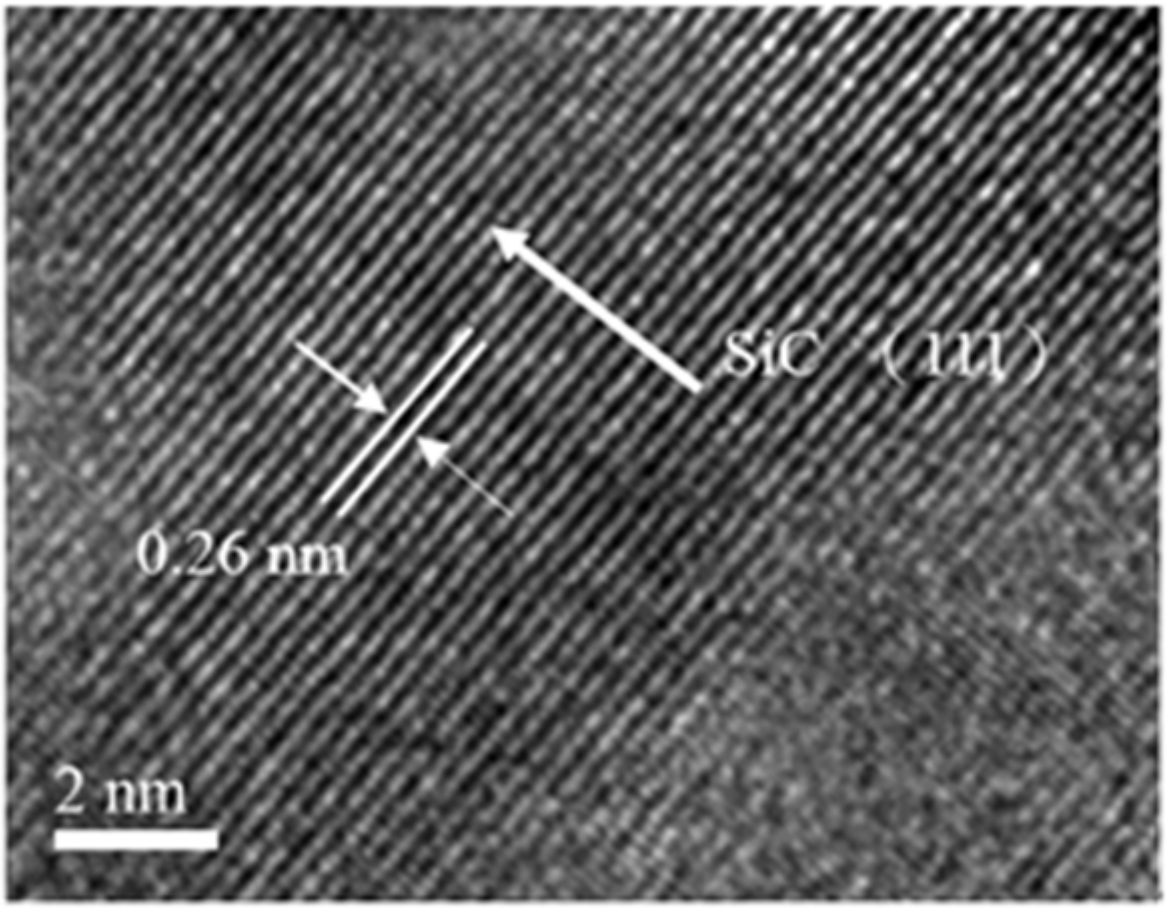

Figure 21

Crystal lattice of SiC